Journal of Perceptual Imaging® 5: 000501-1–000501-18, 2022.

The Impact of Optical and Geometrical Thickness on Perceived Translucency Differences

Davit Gigilashvili[1,▲], Philipp Urban[1,2,▲], Jean-Baptiste Thomas[1,▲], Marius Pedersen[1,▲], Jon Yngve Hardeberg[1,▲]

[1]*Norwegian University of Science and Technology, Department of Computer Science; Gjøvik, Norway;* [2]*Fraunhofer Institute for Computer Graphics Research IGD; Darmstadt, Germany*
E-mail: davit.gigilashvili@ntnu.no

Abstract. *In this work we study the perception of suprathreshold translucency differences to expand the knowledge about material appearance perception in imaging and computer graphics, and 3D printing applications. Translucency is one of the most considerable appearance attributes that significantly affects the look of objects and materials. However, the knowledge about translucency perception remains limited. Even less is known about the perception of translucency differences between materials. We hypothesize that humans are more sensitive to small changes in absorption and scattering coefficients when optically thin materials are examined and when objects have geometrically thin parts. To test these hypotheses, we generated images of objects with different shapes and subsurface scattering properties and conducted psychophysical experiments with these visual stimuli. The analysis of the experimental data supports these hypotheses and based on post experiment comments made by the observers, we argue that the results could be a demonstration of a fundamental difference between translucency perception mechanisms in see-through and non-see-through objects and materials.* © *2022 Society for Imaging Science and Technology.*
[DOI: 10.2352/J.Percept.Imaging.2022.5.000501]

1. INTRODUCTION

Translucency is one of the major appearance attributes, significantly impacting the look of different objects and materials [8, 11]. The ASTM Standard Terminology of Appearance [1] defines translucency as "*the property of a specimen by which it transmits light diffusely without permitting a clear view of objects beyond the specimen and not in contact with it.*" Translucent appearance is usually the result of objects and materials permitting some degree of subsurface light transport. The visual stimulus that evokes the perception of translucency in the human visual system (HVS) is impacted by a multitude of intrinsic and extrinsic factors. Intrinsic factors include the optical material properties found in the *radiative transfer equation (RTE)*; namely, wavelength-dependent absorption and scattering coefficients, wavelength-dependent scattering phase function, and wavelength-dependent index of refraction. The average distance travelled by a photon inside the material before it gets absorbed or scattered is called *mean free path*, which is defined as $1/(\sigma_a + \sigma_s)$, where σ_a and σ_s are wavelength-dependent coefficients of absorption and scattering, respectively. This means that when absorption and scattering coefficients are low, a photon on average travels a greater distance in a straight line within this material. A high absorption coefficient results in fewer photons escaping and exiting the material, while a higher scattering coefficient results in more photons redirected to a different direction, i.e. less of the light structure is preserved and the scene behind the object becomes more blurry or completely visually occluded. The direction to which a photon is redirected to after each scattering event is another important aspect. The distribution of this directionality is given by a scattering phase function. While absorption and scattering coefficients are optical and objectively measurable properties, they affect the subjective sensation of transparency, translucency and opacity. Neither the link among those three perceptual attributes, nor the exact role of absorption and scattering coefficients in the perception process, is fully understood [19, 20].

Materials with a large mean free path can be referred to as *optically thin*, while materials with short mean free path can be referred to as *optically thick*. Objects could look nearly transparent either because of a large mean free path permitted by low absorption and scattering coefficients, or because simply the object is geometrically thin, i.e. the distance that a photon needs to travel through the material is shorter, and consequently, the likelihood of an absorption or scattering event is also lower. Therefore, visual stimuli are significantly affected by both – the geometrical thickness of the object and the optical thickness of the material it is made of.

Finally, certain extrinsic factors also impact translucency assessment by human observers, particularly the conditions under which a given object is observed, such as illumination direction [41] and the color of the surface, a translucent object is placed on [14].

Qualitative and quantitative understanding of translucency perception is an interesting topic in academia and industry alike – 3D printing being a vivid illustration of

▲ IS&T Members.

Received Apr. 4, 2021; accepted for publication Jan. 6, 2022; published online March 7, 2022. Associate Editor: James A. Ferwerda.

2575-8144/2022/5/000501/18/$00.00

the latter. Accurate reproduction of spatially-varying color and perceived translucency have been made possible by the recent advances in multi-material 3D printing [5]. Multi-material 3D printing enables mixing transparent printing materials with opaque colored materials, which considerably broadens the appearance gamut of the printers, i.e. the range of different possible looks of a 3D-printed object. On the other hand, as discussed above, the object's shape and geometry can impact the appearance. This generates a need for a geometry-adaptive adjustment of the printing material mixing ratios when transferring perceived translucency from one shape to another. For proper communication and quality assurance in this process, quantification of perceived translucency is needed, which could be denoted in the form of a joint color and perceived translucency space incorporating perceived color and translucency difference metrics. However, the manner in which translucency difference is perceived by the HVS, and how various factors contribute to that process, remain unanswered to date.

Fleming and Bülthoff [12] have noted that different models of transparency perception (such as Metelli's episcotister model of color fusion [29]) cannot explain the perception of translucency in materials like cheese, milk and wax, as the background is not visible through the object and transparency perception cues (such as X-junctions [2]) are absent. They proposed that the HVS does not invert the optical process of light and matter interaction (*inverse optics* hypothesis [32]) to understand the intrinsic properties of a material, but instead it relies on simple image cues to assess translucency. The potential cues could be the occluded scene seen through the object, if the object is thin enough, either optically or geometrically, and also luminance statistics in particular image regions, when it is not possible to see the background through the material.

Motoyoshi [30] showed that luminance contrast characteristics in non-specular regions of the object could potentially be a translucency cue for the HVS. Nagai et al. [31] have shown that perceived magnitude of translucency correlates well with the local luminance statistics, although the most informative region varies from image to image. Gkioulekas et al. [22] observed that edges contain the essential portion of the information needed for translucency assessment, while Sawayama et al. [34] proposed that rugged surface of the object facilitates discrimination of translucency. Both findings indicate that the parts where a photon needs to travel the shortest distance contain the most of information about material translucence. Moreover, Xiao et al. [41] demonstrated that the Stanford Lucy shape [36] permits visual discrimination of more different degrees of translucency than a simple torus shape, proposedly attributed to its complex shape "*with thick and thin sections and features at multiple scales*". Gigilashvili et al. [18] observed that thin parts increase the perceived magnitude of translucency and could, in some cases, evoke a similar magnitude of perceived translucency as done by optically thinner but structurally (geometrically) thicker objects. Further factors that have been proposed to be affecting the perceived magnitude of translucency are illumination geometry [12, 17, 41] and scattering phase function [23].

Despite these advances, multiple fundamental points are yet to be clarified about perceptual translucency, such as perceptual dimensions of translucency, its relation with transparency and opacity, the extent of so called *translucency constancy* and the definition of the term across different contexts [19]. Urban et al. [39] have recently proposed *A (Alpha)* – a nearly perceptual uniform measure of translucency, which links optical properties of a material with the magnitude of perceived translucency it evokes in humans. *A* is software- and hardware independent, also adjustable according to the object's scale and well-suited for 3D printing applications. The authors used virtual homogeneous materials for the psychophysical experiments, to define the psychometric function. They used the method of constant stimuli, where the anchor pair was composed of optically thin materials with suprathreshold translucency difference shaped as the Stanford Happy Buddha [36]. This study inspired our work and we used similar virtual stimuli and experimental protocol.

In this paper, we hypothesize that:

(1) *Presence of thin parts in the object's shape increases perceived translucency differences.* It has been shown that objects with a complex shape possess a broader range of translucency cues, permit discrimination of more levels of translucency, and fail the constancy of perceived translucency faster [34, 41]. Besides, presence of thin parts affect the magnitude of perceived translucency, as the likelihood for a scattering or absorption event is lower than it is in structurally thicker parts of the same object. Xiao et al. [42] have recently shown that geometrically smooth and geometrically sharp objects made of an identical material differ in perceived translucency.

(2) *Humans are more sensitive to translucency differences in optically thin materials.* The hypothesis is derived from the notion that translucency cues present in see-through and non-see-through objects and materials are essentially different [20]. The background distortion and decreased contrast in it, which are only present in see-through, optically thin materials [13, 35], are stronger indicators of subsurface light transport differences than luminance contrast variations, which is considered as a cue in non-see-through objects.

To analyze these hypotheses and to generate further research hypotheses on the topic, we have conducted two psychophysical experiments under controlled viewing conditions. The objective of the experiments was to identify the distance in absorption-scattering physical parameter space needed for visual discrimination of a suprathreshold translucency difference. The distance was measured psychophysically for different object shapes and was compared among five different regions in the absorption-scattering space.

The preliminary results for the first experiment were reported in Gigilashvili et al. [21]. The article provided the qualitative discussion around *Hypothesis 1* and it proposed *Hypothesis 2*, which inspired the second experiment. This manuscript reports the results of the second experiment, extends the work by quantitative analysis of both hypotheses and by quantifying shape differences in terms of surface-to-medial-axis histograms. Although the preliminary results for one of our two experiments (reported in [21]) revealed some indications that the presence of thin parts increases perceived translucency differences, the major observation was that human observers are more sensitive to suprathreshold translucency differences in optically thin materials. The entire experiment was based on an optically thin anchor pair, which was compared with both optically thin, as well as optically thick test pairs. This raised a concern about optically thin anchor pair as an universal and objective measure for suprathreshold translucency difference. Therefore, we replicated the experiment with an optically thick anchor pair. In-depth analysis of both experiments, as well as a comparison between the two is reported in the subsequent sections.

Our major contributions in this paper are the following:

- We experimentally study how an object's shape, namely, structural (geometrical) thickness and presence of thin parts, impacts perception of translucency differences between materials.
- We experimentally test the hypothesis that the HVS is more sensitive to variations in scattering and absorption coefficients in optically thin materials than in optically thick ones.
- We comment on the validity of A differences (proposed by Urban et al. [39]) across variations in shape.
- We propose new hypotheses for translucency perception research.

2. METHODOLOGY

2.1 *Objective*

The primary objective of *Experiment 1* was to identify whether geometrically thin parts increase the magnitude of perceived translucency difference between two materials. *Experiment 2* was inspired by the results of *Experiment 1*. It was conducted to determine how sensitivity to translucency differences depends on the optical thickness of the materials.

2.2 *Experimental Design*

In order to determine suprathreshold translucency differences for each object's shape, the method of constant stimuli has been used [10]. This is a popular method for determining suprathreshold color differences [3, 38], and has been used for interpreting translucency as well [39, 40]. The anchor pair, which consists of two Buddhas with a suprathreshold translucency difference and remains fixed throughout the whole experiment, is compared with a test pair. The test pair consists of two similarly-shaped objects – one control point (CP) and one respective test sample (see Section 2.3.1).

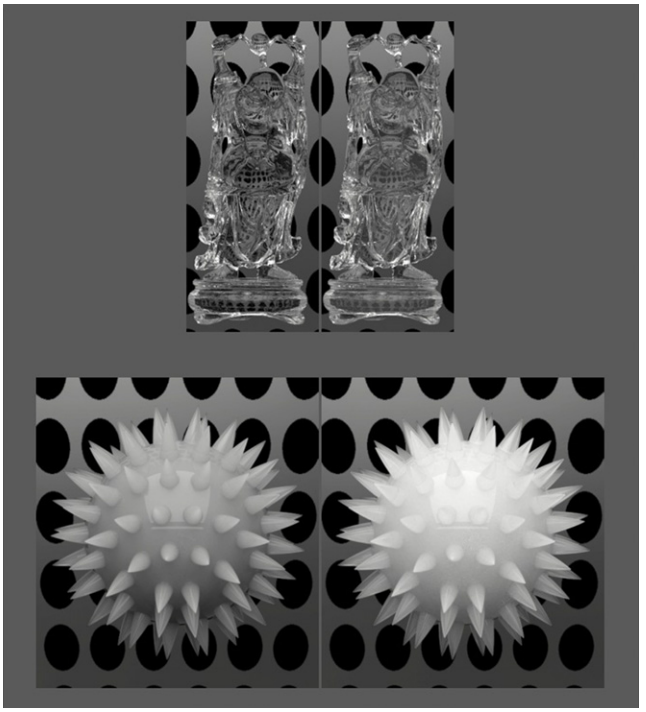

Figure 1. An example of the comparison shown during the experiment. The top pair represents a see-through anchor pair with a suprathreshold translucency difference. The bottom pair is a test pair which consists of a control point (left) and test sample (right) materials. The task of the observer is to determine which pair has a larger translucency difference.

The task of an observer is to identify which pair has larger difference in perceived translucency. Each CP is compared with different test points that are sampled in four different directions, in the absorption-scattering space. The objective is to identify, how far we need to depart from the CP in each direction in the absorption-scattering space, to obtain the translucency difference similar to that of the anchor pair. The following instruction was given "*Please, select a pair, either a top, or a bottom one, with higher translucency difference*" without explicitly defining translucency. The observers had to use arrow keys of a standard keyboard to select the respective pair. The pairs were displayed atop each other on a neutral gray background. The two images within a pair were separated with a 3-pixel gap. The position of the pairs (whether the anchor is the top or the bottom one) and within each pair (left or right) was randomized. A sample comparison from the experiment is shown in Figure 1. The only difference between *Experiment 1* and *Experiment 2* was the anchor pair, as they were based on see-through and non-see-through anchor pairs, respectively. All other procedures were identical between the two experiments. 5 CPs $\times$ 4 directions $\times$ 5 samples per direction $\times$ 5 shapes, amounted to 500 comparisons per experiment.

2.3 *Stimuli*

We used a set of simple virtual materials, similar to those used by Urban et al. [39]. All stimuli were presented on a calibrated display using a *Virtual Viewing Booth* [39]. The

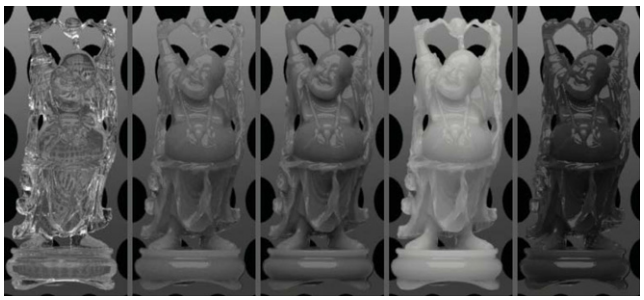

Figure 2. Control points. Five CPs have been selected in the absorption-scattering space. The CPs 1-5 from left to right, respectively, illustrated on the example of Happy Buddha shape.

CIE D65 diffuse light source is located on the ceiling, which is typical to what we encounter on a daily basis – both indoors and outdoors (refer to [39] for the full specification of the *Virtual Viewing Booth*). We used Monte-Carlo Bidirectional Path Tracer in the Mitsuba Physically-based Renderer [25] to solve the RTE. The minimum path depth was set to 20 and "Russian Roulette" termination was deployed afterwards.

In order to keep the degrees of freedom within the manageable range, identical surface roughness, scattering phase function and indices of refraction were used for all objects. In particular, we used perfectly smooth microfacet-scale surface roughness and isotropic phase function. The refractive index of the outer medium was set to 1 (vacuum), while that of materials was fixed to 1.3, which is a characteristic of water and typically has small Fresnel reflection [39] (large portion of the light is refracted towards the subsurface).

2.3.1 *Test Pairs*

We have varied only three parameters: absorption and scattering coefficients, which were assumed to be wavelength-independent, and shape. We selected five control points (CPs) in absorption-scattering physical parameter space, covering both optically thin (CP1) and optically thick (CPs 2–5) regions. The materials corresponding to the CPs are illustrated in Figure 2. All different absorption-scattering coefficient pairs used throughout the experiment are given in Table I. For each CP, five sample points were selected on each of the four directions in absorption-scattering space (examples are illustrated in Figure 3). For each direction, we ensured that perceived translucency difference between a CP and at least one sample point was smaller than that of the anchor pair, and larger for at least one other sample point. In the selection process, we relied on *Alpha* differences ($\Delta A = 0.1$ produces a suprathreshold translucency difference, which is close to the just-noticeable difference [39]) and visual inspection in a trial-and-error manner conducted by the authors of this paper (external observers did not participate in this process). The exact procedure we used for sampling in different directions is given below:

(D1) 1-dimensional change – increasing scattering coefficient for CPs 1 and 2; decreasing scattering coefficient for CPs 3, 4 and 5; fixed absorption. Marked yellow in Table I.

(D2) 1-dimensional change – increasing absorption for CPs 1 and 2; and decreasing absorption for CPs 3, 4, and 5; fixed scattering. Marked orange in Table I.

(D3) 2-dimensional change – increasing absorption and scattering for CPs 1 and 2; decreasing absorption and scattering for CPs 3, 4, and 5. All points were located on a straight line defined as $\sigma_a = \sigma_s$ for CPs 1–3; $\sigma_a = \sigma_s - 116$ for CP 4; and $\sigma_a = \sigma_s + 116$ for CP 5, where σ_s is scattering, and σ_a is absorption. Marked green in Table I.

(D4) 2-dimensional change – increasing absorption and decreasing scattering with points located on the following straight lines: $\sigma_s = -\sigma_a + 9$ for CP 1; $\sigma_s = -\sigma_a + 155$ for CP 2; $\sigma_s = -\sigma_a + 301$ for CP 3; and $\sigma_s = -\sigma_a + 185$ for CPs 4 and 5 (blue in Table I).

These materials were shown in five different shapes: a Happy Buddha from the Stanford 3D Scanning Repository [36] (identical to the one used in [39]), a perfect sphere (with a radius of 5 cm) and three additional spheres with 100 spikes of varying length and thickness (illustrated in Figure 4). Adding spikes introduces geometrically thin areas on a compact spherical object that are easier for a photon to go through and that according to our hypothesis increases the magnitude of perceived translucency differences.

2.3.2 *Anchor Pairs*

Both anchor pairs were composed of Buddha figures with suprathreshold translucency differences. The optically thin anchor pair (see-through) was identical to the one used in [39], using scattering coefficients of 0 cm^{-1} and 1.5 cm^{-1}.

The optically thick anchor pair (non-see-through) was composed of Buddha figures with similar absorption coefficient equal to 77.5 cm^{-1} and different scattering coefficients equal to 77.5 cm^{-1} and 142.48 cm^{-1}, respectively (all absorption and scattering coefficients in this work are expressed in cm^{-1} scale; for simplicity's sake, they will be referred as numbers only throughout in the paper). In order to ensure that the perceptual difference in optically thick anchor pair was equivalent to that of the original anchor pair, we relied on the results from *Experiment 1*. Namely, one Buddha of the non-see-through anchor pair was identical to CP2 (because T50 distances were measured from CPs only), and the second one was T50 distance away from it, as per *Experiment 1* (T50 distance is the distance to the point in the absorption-scattering space, dubbed "T50 point", which by 50% of the observers is considered to be more different from the CP, than the perceived translucency difference of the anchor pair). Our selection was also supported with nearly matching ΔA in the two pairs (0.10 and 0.08, for see-through and non-see-through anchor pairs, respectively). Both anchor pairs are shown in Figure 5.

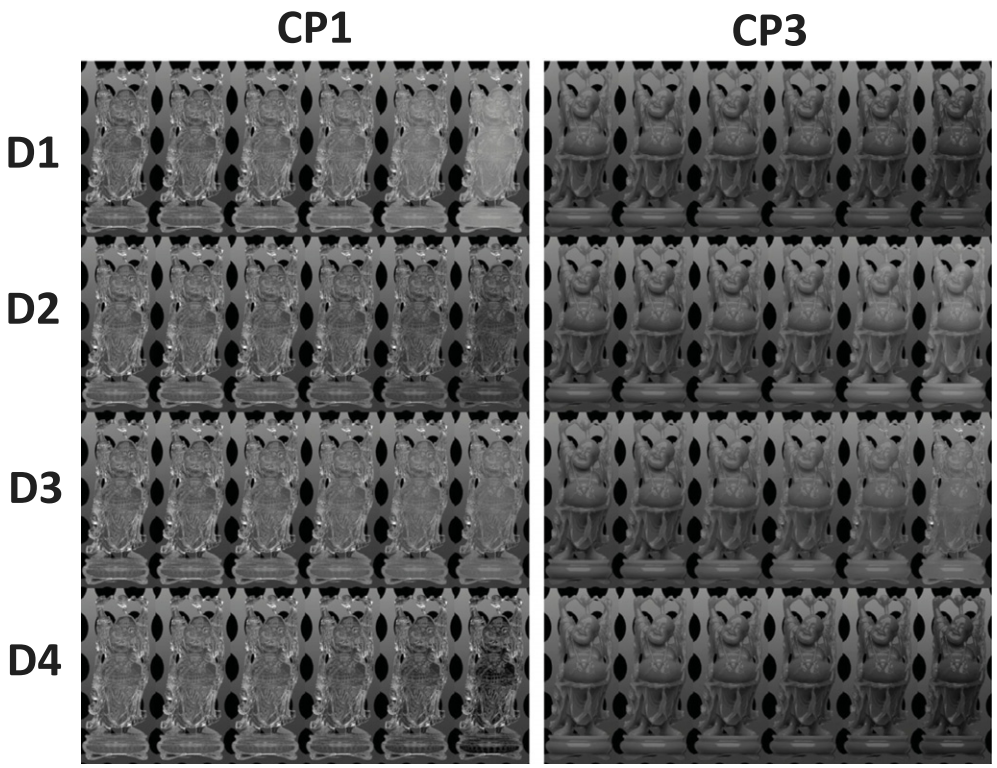

Figure 3. Examples of the stimuli. The stimuli are illustrated on the Buddha shape, and CPs 1 and 3. The control points are shown in the first columns of all rows, while each row illustrates samples in a given direction. For CP1, the rows correspond to increasing scattering (D1), increasing absorption (D2), increasing both absorption and scattering (D3), and decreasing scattering – increasing absorption directions (D4), from top to bottom, respectively; For CP3, the rows correspond to decreasing scattering (D1), decreasing absorption (D2), decreasing both (D3), and decreasing scattering – increasing absorption directions (D4), from top to bottom, respectively; We can observe that in optically thin region (CP1), the amount of background distortion and contrast vary, which are supposedly used as cues to translucency; For optically thicker material (CP3), no shine-through cues are visible (unless the both coefficients are decreased considerably, as in the rightmost column of the third row) and change in absorption and scattering modulate the lightness of the material – absorption and scattering making the shade darker or lighter, respectively.

Table I. Materials used for rendering the stimuli. The experimental stimuli differ with their locations in the absorption-scattering space. The table summarizes absorption and scattering coefficients used to render these stimuli. Each control point is represented by a pair of columns. Control point coordinates are marked red, while the test samples in four different directions are labeled yellow, orange, green, and blue cells, respectively.

Control Point 1		Control Point 2		Control Point 3		Control Point 4		Control Point 5	
Scattering	Absorption	Scattering	Absorption	Scattering	Absorption	Scattering	Absorption	Scattering	Absorption
4.5	4.5	77.5	77.5	150.5	150.5	150.5	34.5	34.5	150.5
4.7	4.5	78	77.5	148	150.5	145	34.5	30	150.5
6	4.5	82	77.5	141	150.5	135	34.5	20	150.5
7	4.5	90	77.5	121	150.5	125	34.5	15	150.5
10	4.5	110	77.5	100	150.5	110	34.5	5	150.5
20	4.5	130	77.5	71	150.5	95	34.5	0	150.5
4.5	4.8	77.5	80	150.5	148	150.5	30	34.5	145
4.5	6	77.5	100	150.5	140	150.5	23	34.5	130
4.5	8	77.5	120	150.5	125	150.5	15	34.5	120
4.5	12	77.5	150	150.5	100	150.5	7	34.5	100
4.5	20	77.5	200	150.5	80	150.5	0	34.5	50
4.7	4.7	85	85	140	140	146	30	30	146
5.5	5.5	95	95	100	100	139	23	25	141
7	7	100	100	80	80	131	15	17	133
9	9	140	140	60	60	123	7	10	126
12	12	1000	1000	25	25	116	0	0	116
4.3	4.7	72	83	145	156	148	37	30	155
4	5	65	90	135	166	140	45	25	160
3	6	50	105	120	181	130	55	17	168
2	7	40	115	110	191	120	65	10	175
0	9	30	125	90	211	105	80	0	185

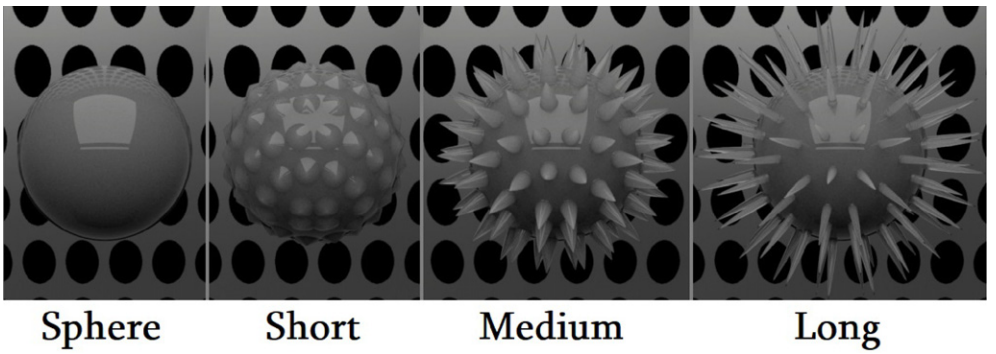

Figure 4. Sphere and spiky spheres. We added spikes of varying length and thickness to a sphere to generate three additional shapes. The spikes are geometrically thin and might contain significant information for assessing translucency differences. The material of the illustrated objects corresponds to that of CP 2 ($\sigma_a = 77.5$; $\sigma_s = 77.5$).

Figure 5. Anchor pairs. A see-through anchor pair (left) was used in Experiment 1, while Experiment 2 was based on the one that does not permit see-through (right).

2.4 *Analysis*

2.4.1 *Probit Analysis and T50 Distances*

We are interested to learn how far we need to move from the CP in the absorption-scattering space to notice the difference in perceived translucency. As discussed above, we hypothesize that this distance depends on the shape and it is shorter for the objects with thin parts. We also hypothesize that this distance is shorter for optically thin see-through materials.

First of all, we conducted a frequency analysis of the observer responses to observe how they change as the Euclidean distance in the absorption-scattering space increases between a CP and a test sample. Afterwards, we fit a Probit binomial model for each direction to estimate the Euclidean distance to the T50 point in the given direction. The distance to the T50 point a.k.a. the point of equal opportunity (or the point of subjective equality), is the distance between the sample and CPs at which 50% of the observers consider the test pair difference smaller than that of the anchor pair, while the other 50% consider it larger. In this case, we consider the difference in the test pair to be equal to suprathreshold translucency difference. The fitting was conducted using MATLAB's Probit link function in generalized linear regression (*glmfit()*).

The Probit model is suitable as the dependent variable is binary ("different from the anchor pair" or "not different from the anchor pair"). Although logistic regression could also have been used in this scenario, we opted for the Probit analysis in order to make our results comparable with that of Urban et al. [39]. The predictor variable is the Euclidean distance in the absorption-scattering space producing the estimate of the proportion of the observers that judged test pair to have a larger translucency difference than the anchor pair. We then invert the problem to get the Euclidean distance corresponding to 0.50 proportion. An example of the fitted curve is illustrated in Figure 6.

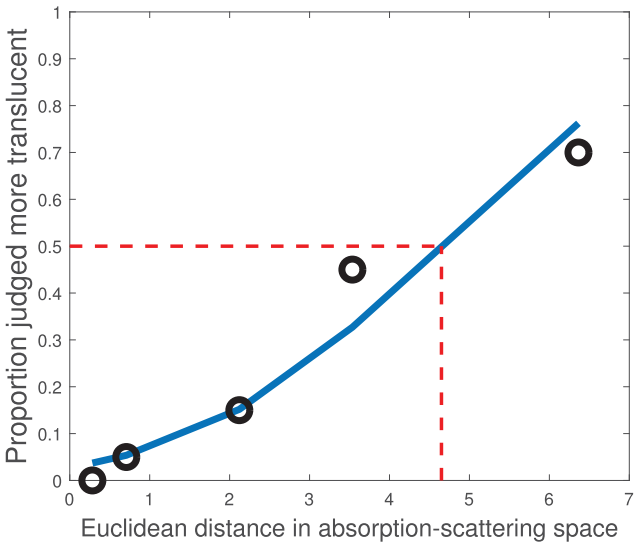

Figure 6. Probit fitting. The Probit fitting on the example of Buddha shape, CP1, the diagonal direction of increasing absorption and decreasing scattering. The black circles mark the test samples that are compared with the center point. The horizontal axis shows how far away the test samples are from the center point and the vertical axis shows the proportion of the observers that considered the test pair difference for a given sample point larger than that of the anchor pair. The fact that four test samples are below the T50 point, indicates that test sample selection might not have been optimal due to the differences between the authors' and naïve observers' judgments, which is later discussed in the Limitations section.

Afterwards, χ^2 goodness-of-fit test was conducted with α set to 0.05. Identification of the T50 point with high confidence has not always turned out possible. In some cases, the estimations failed a goodness-of-fit test ($\alpha > 0.05$), while in some other cases, the estimated position was physically implausible (e.g. negative absorption or scattering). It is worth highlighting that the fitting procedure provides an estimate of the T50 point positions, even if it fails the goodness-of-fit test. We call these *potential* positions for T50, and dashed-lines, instead of solid ones are directed toward them in Figure 7. Finally, we analyzed how these distances to T50 points vary among different shapes, CPs and directions. The distances to T50 points is a measure we use to quantify "sensitivity" to suprathreshold translucency differences. For instance, if for a bumpy sphere we need a smaller change in absorption and scattering coefficients than for a perfect sphere, so that 50% of the observers judge the corresponding translucency difference to be larger than that of the anchor pair, then we can deduce that the observers are more sensitive to the changes in absorption and scattering coefficients when comparing bumpy spheres.

2.4.2 *Quantifying Shape*

Rank order analysis of the T50 distances among different shapes only offers a general, conceptual discussion of the impact. We used a shape descriptor to quantify the geometrical characteristics of a shape and correlate it numerically with the T50 distances. We calculated surface-to-medial-axis distances [4, 33] and used its histogram statistics to characterize the shape. The medial axis is the topological skeleton of a shape. Surface points in thick and thin parts of the object are, respectively, further and closer to the medial axis.

2.5 *Observers*

27 observers including three co-authors of this article have participated in the experiments. 18 were male and 9 were female, representing 20 different nationalities. The median age was 31 years with standard deviation equal to 10.97. All of them passed a Snellen visual acuity test to make sure that they had normal or corrected-to-normal vision. As wavelength-independent absorption and scattering yield grayscale stimuli, color vision of the observers was not tested. 21 observers had a background in color science, imaging, vision, material appearance or related fields.

As the *Experiment 2* was conceived after the preliminary analysis of the *Experiment 1*, there was a considerable temporal gap between the start of the two experiments, which made it impossible to have all observers available for the both experiments. Besides, in order to avoid exhaustion and lack of concentration among observers, lengthy experiments have been avoided and 1000 comparisons (500 comparisons per experiment) were distributed over three different sessions, where not all observers were able to participate. Eventually, each comparison has been assessed by 20 observers. No comparisons were assessed by all observers, and not all observers were shown all comparisons. 23 participants assessed comparisons from both experiments, while 4 observers assessed comparisons from *Experiment 1* only.

2.6 *Display and Viewing Conditions*

Both experiments were conducted on the same color-calibrated display and under the same viewing conditions. The stimuli were displayed on a 24.1 inch EIZO ColorEdge CG246 LCD, which was calibrated to CIE D65 white point with gamma equal to 2.2. Konica Minolta CS-2000 spectroradiometer was used to measure the luminance of the monitor displaying a perfect diffuser patch. The maximum measured luminance was 196 cd/m^2 with 6542 K color temperature. The monitor was warmed up for at least 30 min before each experiment.

The experiment took place in a completely dark room, where the display was the only light source. The distance between an observer and the display was approximately 60 cm. 148 × 348 pixel images were used to display the anchor pairs, occupying 3.81° of the visual field horizontally and 8° vertically. The height of the test pair images was 348 pixels, while the width varied depending on the shape. The largest image with 348 × 348 pixels was used to display spheres with the longest spikes. All test pairs occupied 8° vertically and 6.20°, 6.48°, 8.10°, and 8.96° horizontally, for spheres with no, short, medium and long spikes, respectively (we ensured that the distance from the objects to the vertical edges of the image was the same for all shapes; cropping the non-occluded part of the background is unlikely to have affected the results, as the point-wise difference in these regions is negligible).

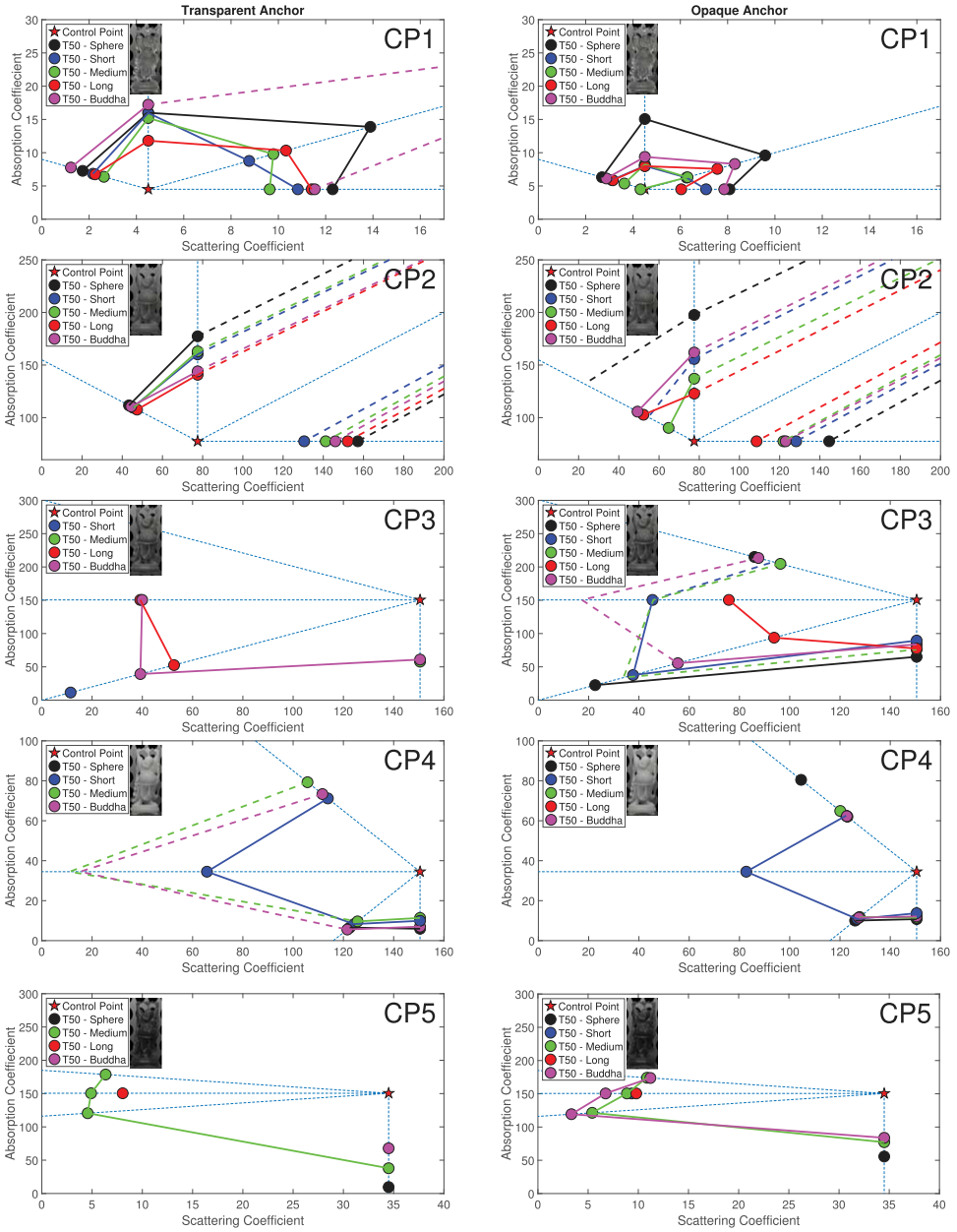

Figure 7. The results. The location of the T50 points for each CP and type of anchor (left column – transparent; right column – opaque). Only the T50 points that are physically plausible and passed goodness-of-fit test are shown and connected with solid lines. If the estimate failed a goodness-of-fit-test but it is within a plausible range, dashed-lines are directed towards its potential position. The Buddhas shown next to the legend illustrate the CP material.

3. RESULTS

3.1 *Results for each Control Point (CP)*

The results for all individual CPs and types of anchor are illustrated in Fig. 7.

For CP1, which is optically thin and see-through, the T50 point is determined in the vast majority of the cases. When non-see-through anchor pair was used, the T50 point was determined for all objects in all directions. The distances from the control point are generally short and they are shorter when these see-through test pairs are compared with a non-see-through anchor pair. The distance is usually largest for a spherical shape, while no clear difference is visible among other shapes.

For CP2, the distances are usually larger for a spherical shape, while no clear trend emerged for other shapes. Interestingly, T50 point is never determined for the more opaque direction ($\sigma_a = \sigma_s$) and the difference in both anchor pairs was usually judged larger than the difference between a CP and a test sample with higher absorption and scattering. This implies that when the mean free path is sufficiently short, shortening it further does not yield any perceptual difference.

Table II. Determined and missing T50 points. Green cells indicate that T50 point was reached and determined with high confidence for a given shape, CP and direction, red cells indicate that it was not. The rows marked *D1* and *D2* correspond to one-dimensional change in scattering and absorption directions, respectively; *D3* and *D4* correspond to the 2-dimensional change. The left and right halves of the diagram illustrate results from *Experiment 1* and *2*, respectively. The anchor pair with shine-through cues is referred to as *transparent* and its non-see-through counterpart as *opaque*, for simplicity's sake. The abundance of the red cells is noteworthy for spherical and long-spike shapes. While the former is intuitive and aligned with our hypothesis, the latter is surprising, as we hypothesize that the distance to T50 point is shortest for the object with thin spikes – thus, most likely to reach it with given sample points. Interestingly, for CP2, T50 point was never reached in the optically thick direction (D3). The numbers in each red cell indicate the number of observers (out of 20) that considered the difference between a CP and the sample in a given direction to be larger than that of the anchor pair – leftmost number corresponding to the closest sample point, and the rightmost one corresponding the furthermost one. Observer responses exhibit highly non-monotonic behavior for many of those cases, which to some extent might be attributed to the random noise.

		Transparent Anchor Pair					Opaque Anchor Pair				
		Sphere	Short	Medium	Long	Buddha	Sphere	Short	Medium	Long	Buddha
CP1	D1								7,15,12,16,19		
	D2										
	D3					2,4,5,3,5					
	D4										
CP2	D1										
	D2										
	D3	4,2,3,4,1	1,1,2,2,6	2,3,2,2,7	3,0,1,1,5	2,1,2,3,7	3,1,3,2,6	3,3,3,3,6	4,4,6,5,10	4,7,3,7,9	0,2,2,2,5
	D4						3,10,8,5,11	4,12,13,12,11			
CP3	D1	2,0,5,3,5	0,2,3,4,4	4,1,5,4,6			2,5,2,3,5		3,4,6,6,8		2,2,1,6,5
	D2	3,2,6,4,4	3,5,6,6,6		2,1,4,3,5						
	D3	1,1,0,3,6		2,5,5,3,5					5,9,7,6,12		
	D4	1,4,5,2,6	3,6,5,8,7	3,4,4,6,8	6,5,2,2,5	1,2,5,4,5		2,7,11,9,8		11,5,3,4,4	
CP4	D1	2,2,3,2,3		3,2,1,3,5	4,1,6,3,6	2,2,4,4,4	1,2,0,5,1		3,1,4,6,3	5,0,4,2,1	3,1,3,2,2
	D2				5,4,4,10,5					4,2,7,4,9	
	D3				4,2,4,6,7					3,4,3,8,7	
	D4	3,4,2,7,7			5,6,8,8,10						
CP5	D1	3,3,5,3,3					2,4,6,4,7				
	D2		9,8,6,14,8		4,6,5,5,9			11,11,12,13,12		4,9,10,6,8	
	D3	2,0,2,2,5	7,8,8,3,12		6,7,8,9,11	1,1,3,5,7	0,2,2,5,6	7,7,7,5,10		12,13,12,12,10	
	D4	1,3,5,6,6	7,7,2,2,12		8,8,9,10,12	3,4,6,7,7	0,5,4,9,8	9,11,6,7,12		13,11,11,12,15	

For CP3, the estimated T50 point coordinates for a spherical object have been negative, thus, physically implausible when the experiment was conducted on a see-through anchor pair. Also, T50 is never reached when scattering decreases and absorption goes up. This can be explained with the fact that observers considered all test samples already opaque and increasing absorption, simply affected their lightness, not their translucency cues. However, we cannot rule out that the reason for failure of reaching T50 could be due to improper selection of the sample points, i.e. the range might be too small. Interestingly, this trend changes and T50 points are reached more often when a non-see-through anchor pair is used instead, which can indicate that sensitivity to see-through and non-see-through anchor pairs differs.

For CP4, the distances to T50 points are rather large and generally consistent among all shapes. For a sphere with thin long spikes, T50 was determined only when non-see-through anchor-pair was used. Further observation is that the decrease in absorption leads to more noticeable appearance difference than the decrease in scattering. This could be rooted in the fact that the magnitude of absorption of a CP is considerably smaller than the magnitude of its scattering.

For CP5, similarly to other CPs, T50 distances have been shorter and easier to determine when samples were judged against a non-see-through anchor pair. On many occasions, a scattering estimate has been negative, which can be attributed to the CP's proximity to the scattering axis (i.e. the CP is too close to the axis and it is not sufficiently different from the sample point located on the axis; it is worth mentioning that this is the case when decreasing direction is examined; negative estimates are not obtained if all sample points are in the increasing direction, as for CPs 1 and 2). In both experiments, pairs of objects with thin parts have higher magnitude of perceived translucency difference than pairs of spherical objects. For this CP, the object with the medium-sized spikes has been the best one to detect translucency differences on.

3.2 *General Trends*

On many occasions, T50 distances are neither reached, nor estimated with high confidence. Refer to Table II – if the T50 point was reached for a given CP in a given direction, a respective cell is marked green, otherwise, it is marked red. The table shows that T50 point was not reached 38 times (number of red cells in the respective half of the table) out of possible 100 (5 shapes × 5 CPs × 4 directions) when see-through anchor pair was used and 29 times when the experiment was based on non-see-through anchor pair. As the test pairs have been identical in both experiments, this is an indication that observers are more sensitive to background distortion cues of the see-through anchor pair when comparing it to non-see-through test materials. Additionally, the T50 point was reached for optically thin CP1 in all but one occasion in both experiments.

Most frequently, the T50 point is not reached for the spherical object and for the one with long thin spikes, while it is mostly reached for Buddha and the sphere with medium-sized spikes. A compact spherical object lacks thin parts and respective translucency cues, while Buddha per contra possesses finer details, i.e. broader range of translucency cues (as shown by [41]). These two observations are consistent with our hypotheses. However, the results for a sphere with the thinnest spikes is largely counter-intuitive.

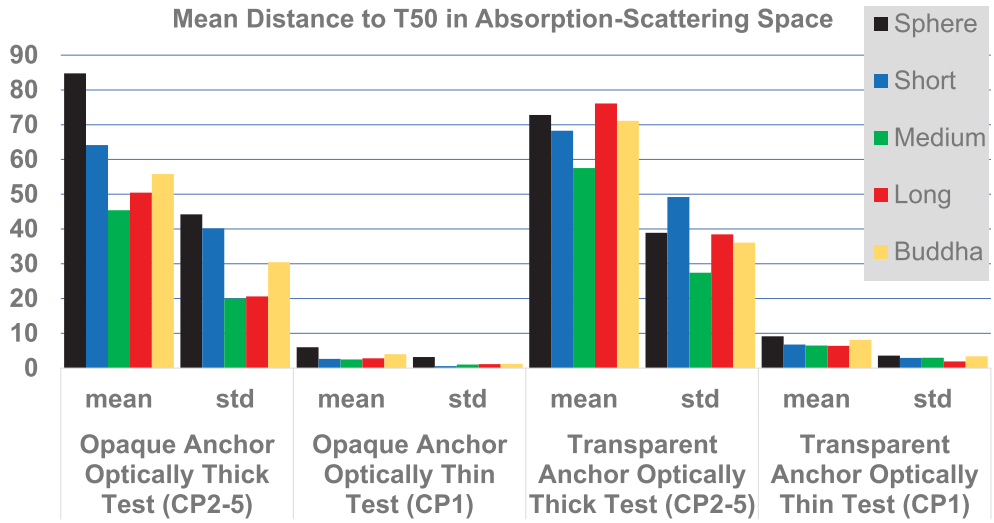

Figure 8. Variation of the mean distance to T50 points in the absorption-scattering physical parameter space across different sets of comparisons. The anchor pair with see-through cues is referred to as *transparent* and its non-see-through counterpart as *opaque*. It is apparent that the distance is shorter when optically thin test pairs are assessed. Also, using see-through anchor pair increases both the mean distance to the T50 point, as well as the standard deviation. For spherical objects the mean distance is usually larger than that of Buddhas and spheres with short- and medium-sized spikes. Only physically plausible estimates which had passed a goodness-of-fit test have been considered. Thus, the information is not available for all T50 points (see 4.8 *Limitations*). A different range of sample points might help us determine more T50 points in the future. However, all cases of failure in T50 point estimation, was because all sample pair differences were considered smaller than that of the anchor pair, and not because all of them were deemed larger. Hence, we anticipate that more T50 points can be determined if and only if the span of the sample points is broader, which will further increase the mean distance to T50 point for optically thick test pairs, and will not essentially change the fact that distances to T50 are shorter in optically thin regions.

While the luminance gradient characteristic for translucency is visible on wider and thicker medium-sized spikes, it might be harder to detect on thinner spikes due to contrast sensitivity limitations – they simply occupy a smaller portion of the field of view (e.g. ref. to Fig. 4). A second explanation for this result can be found in the remarks made by the observers – some of them noted that the spikes look so different from the spherical core that they thought they were made of different materials and decided to assess just the major body of the object. While these hypotheses deserve further study, the relation between structural thickness and sensitivity to translucency differences is evidently neither straightforward, nor monotonic.

Figure 8 shows the mean distance needed to reach the T50 point for different shapes and materials. We can observe that the distance is considerably shorter for optically thin test materials and also when non-see-through anchor pair was used, being consistent with our hypotheses. Being aligned with our hypothesis, the mean distance to the T50 point is larger for a sphere than it is for Buddha and spiky objects with short- and medium-sized spikes (although not with long spikes). Figure 9 illustrates average *Alpha* distances to T50 points. We can see that ΔA largely accounts for the sensitivity difference between optically thin and optically thick materials. However, shape-specific adjustments are needed.

3.3 *Histogram of Surface-to-medial-axis Distances*

The histograms are shown in Figure 10. The summary statistics of the histograms and how they correlate with the mean T50 distances are given in Tables III–IV, respectively. Mean and median distance to the medial axis, as well as the percentiles, are significantly correlated with the T50 distances, except for the case, when the optically thin anchor pair is compared with the optically thick test pairs. However, standard deviation, skewness and kurtosis turned out to be poor correlates of the psychophysical data. The medial axis of a perfect sphere is its center and the distance to it is equal to its radius, for all surface voxels. This makes it challenging to compare a perfect sphere with other shapes in terms of histogram statistics. The data for spheres has been only considered when a given metric was applicable to spheres.

While these metrics assume a single Gaussian distribution, there are in fact two distributions of thicknesses in spiky objects – the core sphere with larger distances and spikes with shorter distances. We fitted a two component Gaussian mixture model to the histogram and report the ratio between component proportions, as well as the difference and ratio between the means of the two Gaussians. Against our expectations, neither of the three correlated with the observer data. We want to highlight that the accidental similarity in the magnitudes of geometrical thickness and T50 distances can produce high Pearson correlation, while the rank order correlation can still be insignificant (e.g. see the difference between the means of the two Gaussians when optically thin test and optically thick anchor pairs are compared).

4. DISCUSSION AND ANALYSIS

The analysis of the experimental results revealed several interesting trends, which are consistent with our hypotheses as well as with the state-of-the-art in translucency perception

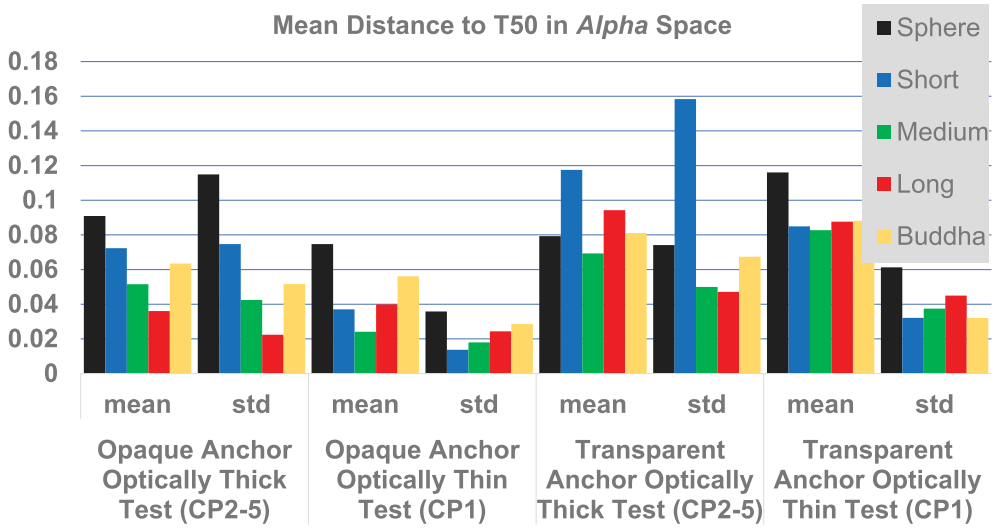

Figure 9. *Alpha* distance to the T50 point. The figure illustrates that ΔA largely accounts for inconsistency between optically thin and thick test samples which was apparent in absorption-scattering space. However, shape-dependent differences remain. As in case of Figure 8, the information is not available for all T50 points (see *4.8 Limitations*).

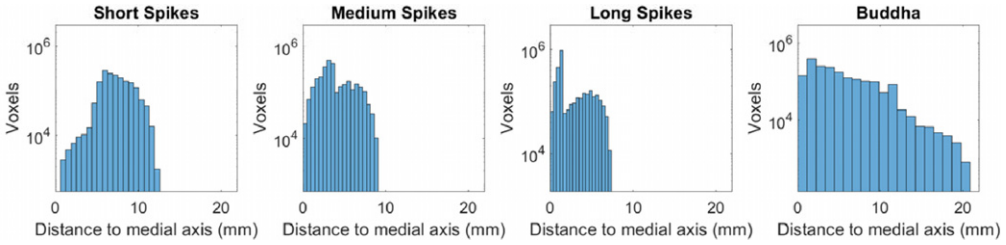

Figure 10. The histogram of surface-to-medial-axis distances. As the physical dimensions of the objects vary, the histograms are not directly comparable in terms of the absolute number of voxels. However, the summary statistics of the histogram provide insight into the overall distribution of thin and thick parts. Thinner and longer spikes lead to a tail in the lower end of the histogram and produce a stronger positive skew.

research. The most significant observations we have made are as follows:

- We have been unable to determine T50 distances in $\frac{1}{3}$ of the cases and poor selection of the sample points could be a possible reason.
- Presence of geometrically thin parts facilitate detection of translucency differences for some materials, but not for others. The correlation between structural thickness and sensitivity to translucency differences can be characterized qualitatively, but quantitative modelling remains beyond reach.
- Human observers tend to be more sensitive towards changes in absorption and scattering properties when the object has see-through cues, as the T50 distances have been reached with considerably narrower span of the sample pairs in the optically thin region.
- In optically thick materials, increasing absorption and scattering did not yield a suprathreshold translucency difference. It seems that we have not been able to increase the luminance contrast any further due to a diminishing return effect.

Table III. The summary statistics of the surface-to-medial-axis histogram. The values are given in millimeters.

	Sphere	Short	Medium	Long	Buddha
Mean	50	7.37	3.88	2.65	4.84
Median	50	7.14	3.44	1.53	3.95
75th Percentile	50	8.67	5.29	4.2	7.14
99th Percentile	50	11.22	8.29	6.88	15.43
Std	0	1.77	1.88	1.86	3.52
Skewness	N/A	0.01	0.56	0.71	1.03
Kurtosis	N/A	3.12	2.51	2.12	3.71
Component ratio	N/A	0.20	0.42	0.81	0.85
Component mean ratio	N/A	0.72	0.45	0.27	0.31
Component mean difference	N/A	2.66	3.45	3.24	4.92

- ΔA, the perceived translucency difference metric proposed by Urban et al. [39] needs to accommodate shape-specific adjustments.

Table IV. The Pearson and Spearman rank-order correlation between the histogram statistics and the mean distance to the T50 point. The Spearman coefficient is given in the parentheses. When $\alpha < 0.05$, the respective estimate is given in a boldface. The first seven statistics assume single Gaussian distribution, while the last three fit a two-component Gaussian mixture model to the data. As in case of Fig. 8, it is worth noting that the information is not available for all T50 points (see 4.8 *Limitations*).

	Opaque Anchor Thick Test	Opaque Anchor Thin Test	Transparent Anchor Thick Test	Transparent Anchor Thin Test
Mean	**0.92** (0.9)	**0.91** (0.5)	0.27 (-0.1)	0.82 (0.9)
Median	**0.92** (0.9)	**0.91** (0.5)	0.26 (-0.1)	0.82 (0.9)
75th Percentile	**0.92** (0.9)	**0.92** (0.5)	0.28 (-0.1)	0.83 (0.9)
99th Percentile	**0.92** (0.8)	**0.96** (0.7)	0.30 (0)	**0.90 (1)**
Std	-0.70 (-0.7)	-0.51 (-0.3)	-0.10 (-0.3)	-0.33 (-0.3)
Skewness	-0.51 (-0.2)	0.73 (0.8)	0.25 (0.6)	0.55 (0.2)
Kurtosis	0.59 (0.6)	0.74 (0.4)	0.02 (-0.2)	0.91 (1)
Component ratio	-0.38 (-0.2)	0.68 (0.8)	0.58 (0.6)	0.43 (0.2)
Component mean ratio	0.63 (0.4)	-0.50 (-0.6)	-0.39 (-0.8)	-0.24 (0.4)
Component mean difference	-0.20 (-0.4)	0.91 (0.4)	0.12 (0)	0.86 (0.4)

4.1 *Missing T50 Points*

In addition to the random human error, which will be discussed later in Section 4.7, there are three primary explanations for failure to determine the T50 points: proximity of the CPs to the axes, improperly selected sample points and non-existence of a T50 point.

In the decreasing absorption and/or scattering direction (e.g. D1 and D3 for CP5), if the CP is not noticeably different from the sample point located on the axis, the estimated T50 point will be negative and physically implausible. This has been most commonly observed for CPs 4 and 5, that have been close to absorption and scattering axes, respectively, ending in negative estimates in decreasing directions. This means that CPs, especially in optically thick regions, should be sufficiently far away from the axes, if decreasing direction is to be studied.

If sample points are improperly selected, and either all or none of the sample pair differences are noticeably larger than that of the anchor pair, the experiment is not adequate for estimation of the T50 points. We have observed that when we failed to identify a T50 point in our experiment, this was because all sample pair differences were deemed smaller than that of the anchor pair. There can be two reasons for this: either the span of the sample points we selected have been too narrow and we had to test the sample points further away from the CP in the absorption-scattering space, or because it is impossible to produce noticeable translucency difference in a given direction and the realistic T50 point does not exist. We have observed that in optically thick regions, many T50 estimations have been unrealistically high and failed goodness-of-fit test. A broader range of sample points need to be studied in the future to identify whether T50 points can be ever reached and whether the reason for failure in this case was the narrow span of the sample points.

4.2 *Impact of Geometrical Thickness*

The T50 distances that passed the goodness-of-fit test have oftentimes been larger for spherical and thicker objects than for those with thin parts. Moreover, on many occasions, the T50 distances have not been determined at all for a perfect sphere, while they had been found for other shapes.

We observed that mean and median surface-to-medial-axis distances have been better predictors of the experimental data than the measures quantifying asymmetry and distribution of thick and thin parts. However, the average thickness of the object does not adequately reflect presence or absence of the thin parts and can depend more on the scale of the object. Our observation is consistent with other research that postulates that the areas where a photon needs to travel shorter distance, such as edges [12, 22] and other fine details on the surface [31, 34, 41], contain the vital portion of the information about material translucence (refer to Figure 11). Although the two optically thick materials are far away in the absorption-scattering space, the pixel-wise difference shows that they differ in thin parts, while remain relatively similar in thick areas.

While this trend is easier to characterize qualitatively, proper quantitative modeling of the impact of shape and geometry seems to range from very difficult to infeasible at this stage. First of all, missing T50 points, possibly due to poor selection of the sample points, might have affected the existing correlation between shape descriptors and T50 distances. More importantly, as long as we do not know exactly which image regions the HVS relies on and how it weights the luminance information present in the image, we are not able to construct a shape descriptor that will correlate well with the perceived translucency differences. For instance, the thinnest spikes, against our expectations, turned out counter-productive in assessment of translucency differences. Moreover, a histogram of surface-to-medial-axis distances is viewpoint-blind and accounts for all spikes of the shape. However, we do not know, whether they are equally important [31], as for instance, the spikes located on the backside of the object might have a negligible role. However, this limitation is less important in real-life scenarios, as humans can interact with the objects and inspect them from all different geometries [18].

Thin parts that are represented as bumps considerably affect the surface topography. They generate shadows and provide additional cues about the surface geometry of the object (refer to Figure 12). Although the respective objects are made of the identical materials in both pairs, the difference becomes more apparent in the right pair, as the bumps of an optically thick material produce sharper shadows than its optically thinner counterpart. Similar image contrast resulting from a surface relief has already been shown by Xiao et al. [42] to be diagnostic for optical thickness of the material. Marlow et al. [28] have demonstrated that when surface and shading co-vary (as in the right image of the right pair in Fig. 12), the material is perceived as opaque, and when they do not, perception of translucency is evoked (left image in the right pair, Fig. 12). However, a simple

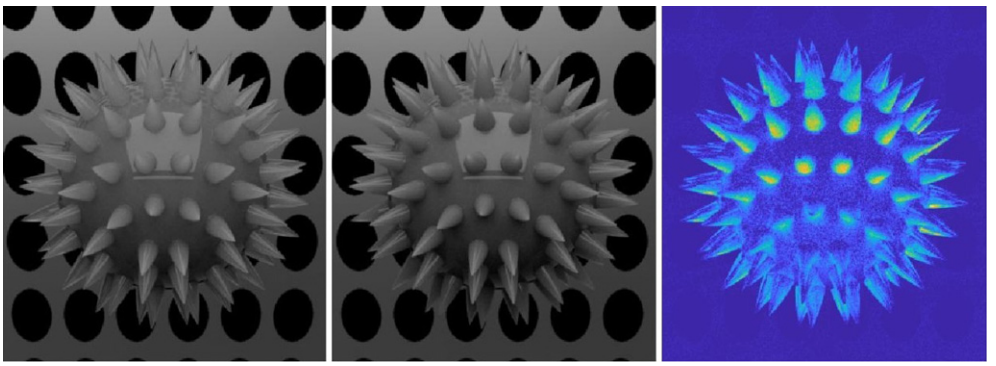

Figure 11. Pixel-wise difference. σ_a and σ_s equal to 77.5 in the left image, and to 1000 in the middle one. The absolute pixel-wise differences between the two are shown in the rightmost 256-level Parula pseudocolor image, where darker blue corresponds to the lowest, and yellow to the largest difference (scaled with a factor of 4.72 for visualization's sake). The maximum absolute difference (before scaling) is 54. Regardless the considerable difference in optical properties, the thick parts remain relatively similar, while the difference is manifested in thin spiky regions.

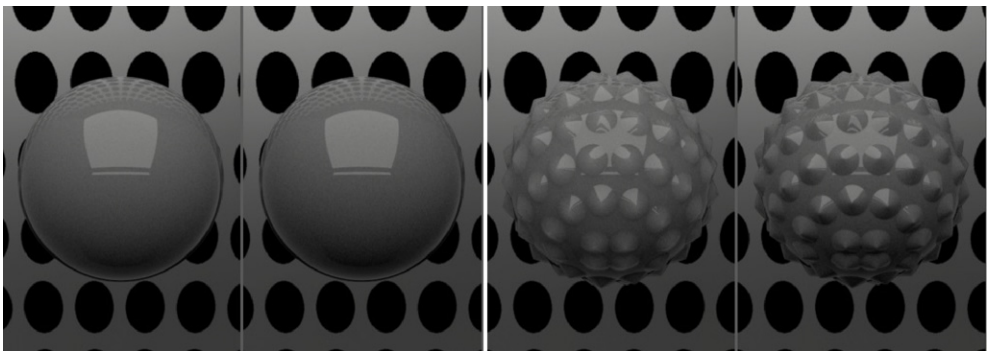

Figure 12. Bumps increase perceived translucency difference. σ_a and σ_s equal to 77.5 in the left images of the both pairs (CP2) and to 1000 in the right ones. Regardless the considerable distance in absorption-scattering space, spheres look nearly identical. The difference becomes more apparent for bumpy objects, as the bumps produce sharper shadows when the material is optically thicker. The figure is reproduced from [15].

spherical shape with no concavities or bumps leaves less room for observing this kind of surface-shading co-variance and leaves more room for interpretation. This may have implications for material appearance research. If a sphere lacks translucency cues, it may be a bad idea to have it as a shape of choice in psychophysical experiments, being consistent with [23].

As the HVS supposedly relies on low level image cues for assessing translucency [12], we believe that careful analysis of the image structure in future works will provide answers as to why geometrical and optical thickness affect perceived translucency differences. It has been proposed that the most informative parts about translucency are edges and thin parts (as shown in Fig. 11), as well as the concavities and convexities that are shadowed in opaque materials and lighter in translucent ones (as shown in Fig. 12) [20]. Although the in-depth analysis of the image statistics is beyond the scope of this work, in Figure 13 we demonstrate how the difference in luminance distribution varies across shapes and optical thickness levels. The figure shows that the pixel-wise difference is larger in optically thin materials, even though the Euclidean distance in the absorption-scattering space is shorter than for illustrated optically thick pairs. For optically thick materials, the difference is smaller and exhibited near the concavities (thin parts) only.

4.3 *Impact of Optical Thickness*

We have observed that when the magnitude of absorption and scattering is low, a smaller change is needed in absorption and scattering properties to notice a translucency difference. This observation is consistent with the findings by Urban et al. [39] and is accounted for by A (see constant A curves in Fig. 3 of [39]). This fact is also consistent with Stevens' law [37] (similarly to [40]) and involves important implications for translucency perception research. Seemingly, the HVS is more sensitive to background contrast and background blur cues present in see-through objects and materials [35] than it is to luminance contrast variation, which proposedly is a translucency cue for objects and materials that do not permit seeing through [12, 22, 26, 28, 31, 41]. See-through cues overtake and outweigh luminance contrast variation cues when both are present. This has the following implications:

- The perceptual mechanisms of assessing see-through and non-see-through objects and materials might be fundamentally different. Therefore, they should be

studied independently – not just in comparison with one another. For instance, when the method of constant stimuli is used, the anchor pair should be selected with care and with full consideration of the corpus of the test pairs.

- This is important for material design both in 3D printing and computer graphics applications. In addition to the fact that this observation will affect material mixing ratios for perceived translucency matching, we hypothesize that the HVS is more sensitive to unintended artifacts when the material is optically thin.

The observers noted in the post-experiment interviews that they relied on background distortion in see-through images, while there was hardly any cue apart from lightness in non-see-through objects and materials. Several observers noted that they always considered the difference in the see-through anchor pair to be larger, because "*the test pair was composed of two opaque materials, meaning that both objects in a pair had zero translucency and thus, were not different by translucency*". To some the test pairs look like "*two fully opaque billiard balls with two different colors*". This supports the proposal by Fleming and Bülthoff [12] that the HVS has poor ability to invert optics. It also seems that if the mean free path is very short, subsurface light transport is not noticeable at all. However, it remains an interesting open question why observers relied on lightness or brightness as a translucency cue. Lightness is natural to highly scattering media and it is characteristic to many translucent materials, such as snow and milk. Therefore, we cannot rule out that lightness itself is a cue for perceived translucency. Geometric information [28] can be important if the surface geometry is complex. For instance, observers might have compared lightness of the spikes, when they were present. However, for simple shapes, such as spheres, regional variation of the luminance distribution is minimal. This can explain why some observers use global mean luminance for assessing translucency, while others simply consider the material to be opaque.

4.4 *Interaction between Optical and Geometrical Thickness Effects*

We hypothesize that there might be an interaction between geometrical thickness and optical thickness effects. This hypothesis is derived from the notion that background distortion is a strong cue for assessing translucency. However, visibility of the background does not only depend on the optical thickness of a material, but also on its surface geometry. For some object shapes, the background is not visible even if the material is optically very thin (see Figure 14).

4.5 *Moving towards Optically Thick Direction*

The special case of the lower visual sensitivity to absorption-scattering changes in optically thick materials is when both absorption and scattering are increased. In this direction the T50 point was never reached. As discussed above, luminance contrast is a cue used for distinguishing levels of translucency between the objects. While scattering and absorption coefficients are positively correlated with brightness and blackness, respectively [9], if both of them

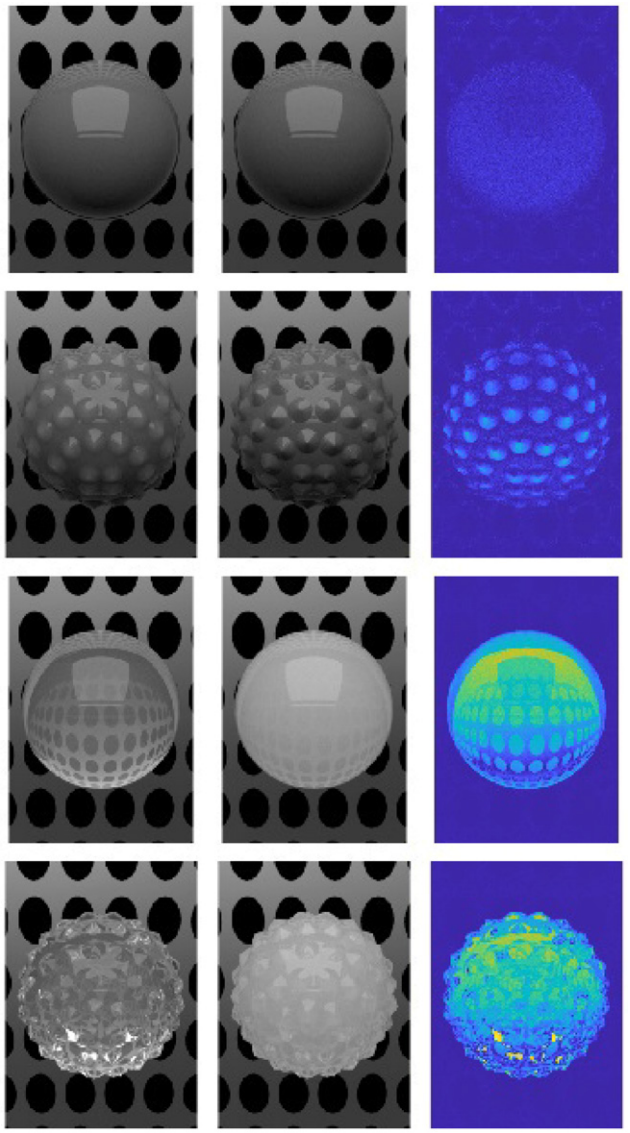

Figure 13. Pointwise differences. The pairs in the top two rows are made of the same two optically thick materials. The third column shows that the absolute pixel-wise difference (scaled with a factor of 2.47; shown in 256-level Parula pseudocolor) in luminance distribution is homogeneous and low for spherical objects, while the difference is large in the areas below the bumps that are darker in an optically thicker material and lighter in an optically thin one. In the bottom two rows, the pairs are made of the same optically thin materials, which have smaller difference in absorption-scattering coefficients than the optically thick pairs in the top two rows. When the background is visible (sphere), its distortion and decrease in contrast are responsible for the most of the pixel-wise differences, but even when the background is not visible due to complex shape (bottom row), the overall intensity difference is still larger than it is for optically thick materials. The maximum absolute difference (before scaling) in the four rows is 47, 52, 82, and 103, from top to bottom, respectively. The HVS might potentially rely on this kind of luminance distribution differences to judge translucency difference.

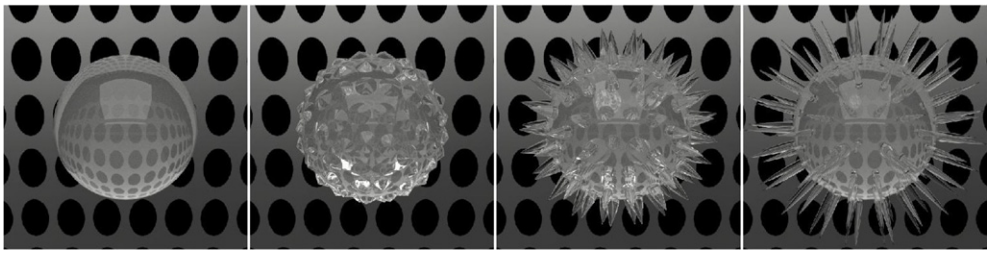

Figure 14. Objects made of optically thin materials are not always see-through. The visibility of the background is strongly affected by object's shape. For instance, a bumpy object (second from the left) does not permit the background to be seen, even though it is made of a transparent material. The figure is reproduced from [21].

are increased equidistantly, there is a diminishing return effect in the resulting luminance contrast and the overall look remains roughly unchanged (refer to the left pair in Fig. 12). This is consistent with the lightness reflectance measurements conducted by Urban et al. [39] (see Fig. 3 in [39]). When the mean free path is short, a photon cannot traverse through a thick body of the material and the penetration depth into the volume is negligibly small. Therefore, shortening the mean free path further does not yield any perceptual difference. However, the mean free path becomes increasingly important as thinner and finer details are introduced in the shape.

4.6 ΔA *as a Measure of Perceived Translucency Difference*

The visualization of the results in absorption-scattering and *Alpha* spaces shows that ΔA accounts for sensitivity differences between optically thin and optically thick regions relatively well. On the other hand, ΔA is not an adequate metric to reflect shape-specific effects on perceived translucency differences. The value of the ideal translucency difference metric should be identical for all shapes and all pairs of control-T50 points. A is a shape-independent material property. However, the arrangement of A in space depends on the shape. The psychometric function used in the definition of A was measured on Buddha shapes [39]. Translucency cues that are present in the Buddhas may be absent in a sphere or other shapes – therefore, their psychometric function may be different. ΔA should be adjusted so that it could accommodate shape-dependent effects on perceived translucency differences.

If we draw a parallel with colors, CIELAB is suitable to quantify color for defined and fixed viewing conditions. However, for color differences, various "parametric factors" need to be taken into consideration [24, 27] (such as distance between the patches, luminance level, presence of texture etc.). For instance, the CIEDE2000 color difference formula [27] can be fitted to parametric factors using *k-values*. We believe that a phenomenologically similar parametric factor for perceived translucency differences is the object's shape, which ΔA should be parametrized for. We hypothesize that the necessary features for parametrization can be extracted from shape descriptors in future work.

Interestingly, T50 distances in the *Alpha* space have not been identical even for Buddha shapes that A was defined on. This can be an indication that besides parametric factors, inter-observer differences also exist.

4.7 *Observer Variability and Random Error*

Further challenge is that the success or failure of the fitting procedure does not depend only on the observers' sensitivity. We cannot assume that the experiment participants are ideal observers, i.e. identical observers always giving an identical response to the identical stimuli. Usually there are sources of variation in the observer responses that we have not accounted for. The most significant source of such kind of noise can be the dissimilarities in internal representations of translucency among different observers. This could potentially explain why the authors' visual judgements in the stimuli selection process did not generalize to a larger group of naïve observers. For instance, the authors being biased by the familiarity with the stimuli rendering process, considered lightness difference as a cue to translucency difference, because they knew surface reflectance had been identical. Naïve observers, unaware of this fact, attributed lightness differences to surface reflectance instead of subsurface scattering ("*two fully opaque billiard balls with two different colors*"). And the fact that different observers assessed different stimuli does not permit us to assess the statistical power of the study. We do not exactly know to what extent the failure to determine T50 points can be attributed to random error in observer responses. Inter-observer variability is accounted for in the Probit model, which assumes that observer responses are normally distributed. The analysis presented above is limited with this assumption. Intra-observer variability can be measured in future studies if the same experiment is repeated with the same observers.

However, examining the raw data might provide deeper insight into the reasons of T50 estimation failure. Table II shows the number of observers that considered the difference between a CP and the test samples in a given direction to be larger than that of the anchor pair. In many cases, observer responses exhibit apparently non-monotonic behavior, which is counter-intuitive, because it is usually expected that a larger difference in subsurface scattering properties yields a larger, or at least similar, but not smaller translucency difference. In this case, random error due to observer confusion and differences in internal representations of translucency are very likely to have played an important role in the failure to

determine a T50 point. For instance, a spherical shape for CP2 compared with an opaque anchor in the D4 direction exhibited high non-monotonicity, which was the reason why the estimated T50 point failed a goodness-of-fit test. Although non-monotonicity can be to some extent filtered away with a method used by Berns et al. [3], collecting more data in the future will enable us conduct bootstrapping, cross-validation and other resampling methods to shed more light to the extent of the noise.

Despite these non-monotonous results, there are particular cases, where the overwhelming majority agreed that the anchor pair difference was larger even for the furthermost sample. For instance, for spherical shape of CP2, all but 1 observer (95% of all observers) considered a transparent anchor pair difference to be larger in D3, while the number decreased for other shapes. In this case, a random error is unlikely to have played a central role. It is possible that the T50 point does not at all exist for a spherical shape, but may exist for other shapes, which was not reached due to ill-selection of the sample points. This is intuitive, because if the mean free path is already short enough for a thick compact object to appear fully opaque, shortening it further will never impact luminance contrast in a perceptually meaningful way, while shortening mean free path might have considerable impact if the object has thin parts.

4.8 *Limitations*

This study comes with multiple limitations that need to be addressed in the future. All experiments were conducted with the same scattering phase function, index of refraction, microfacet-level surface roughness and illumination geometry. These factors are known to modulate perceived magnitude of translucency [12–14, 23, 41] and we cannot rule out that our observations do not hold for other materials. We also assumed wavelength-independent absorption and scattering. Although it has been demonstrated earlier that translucency can be assessed without chromatic information [6, 12], in our daily lives we hardly ever encounter materials with wavelength-independent absorption and scattering; the HVS might not be properly trained to assess this kind of stimuli [6, 7].

The most significant limitation of the study is the fact that T50 points have not been determined in 33% of the cases (38 and 29 times for optically thin and thick anchor pairs, respectively, out of 200 total). Therefore, all observations need to be considered with caution. Ideally, if T50 points were determined for all shapes, anchor pair types, center points and directions, the comparison among them would have been a more straightforward task. The work is based on the assumption that at least one sample point was smaller than that of the anchor pair, and larger for at least one other sample point. If that assumption does not hold, e.g. if all test pair differences are noticeably smaller than that of the anchor pair, the conducted experiment is not a suitable for determination of T50 points. This problem has been observed by Urban et al. [39] who note that T50 estimations, which failed the goodness-of-fit test, "*were characterized by a test sample choice spanning a too small visual translucency difference interval so that many observers found all test pairs in this direction to have a smaller translucency difference than the anchor pair*". We also observed the similar phenomenon – if T50 was not determined, it has been because all test pair differences where considered smaller than the anchor pair by the vast majority of the observers. We admit that our methodology of stimuli selection is limited and neither *Alpha* differences, which are defined on Buddha shapes, nor visual judgements of the authors, can be generalized to all shapes and all naïve observers, respectively. However, this study is motivated by the lack of intuitive perceived translucency space and limited understanding of how absorption, scattering and shape affect perceived translucency differences. This leaves visual inspection by authors in a trial-and-error manner still the most reliable technique, to the best of our knowledge. Moreover, as we hypothesize that perceived translucency differences vary among shapes and the levels of optical thickness, we cannot assume that there exists a unique set of test sample materials that allow estimation of T50 points for all shapes and all anchor pairs at the same time. It might well happen that for one shape, a change in absorption and scattering properties in a given direction never produces larger-than-anchor-pair difference thus, the realistic and physically plausible T50 does not exist for this shape, while this is not necessarily true for another shape. In this case, if T50 point is determined for one shape but not for another one, while both shapes are made of the identical sets of materials, this can be an indication that first shape facilitates detection of translucency differences. Similarly, if the difference between the same test pairs is never considered larger than that of see-through anchor pair, but the very same test pair differences are considered larger than non-see-through anchor pair difference, this might imply that the latter anchor pair difference is smaller than the former. In this case, determining T50 point for one anchor pair and the lack of thereof for another can be also an indication of different sensitivities between them. Furthermore, missing T50 points can still potentially provide insight into differences between optically thin and thick regions. If in optically thin region, T50 distance $T50_{thin} = X$, but in the optically thick region, we have not reached T50 point within the range of Y, where $Y > X$, because all sample pair differences have been deemed still smaller than the anchor pair difference, this indicates that $T50_{thin} \neq T50_{thick}$, and if $T50_{thick}$ exists, then $T50_{thick} > T50_{thin}$.

Whether missing T50 points have not been determined because the span of the test sample materials was too narrow, or because the realistic T50 points for a given shape and direction simply do not exist, is an open question that needs to be addressed in future studies. It is also worth noting that T50 points have been determined for the optically thin CP1 with a considerably smaller range of sample points, while for other CPs, T50 points were not reached even with a broader range of sample points, because the vast majority of the observers considered all sample pair differences to be smaller

than that of the anchor pair. If T50 points exist for those CPs, they should be larger than the maximum span of the current sample points. In this case, even without reaching T50 points with other CPs, it is evident that T50 distances are shorter in optically thin regions.

Besides, our ability to model the correlation between sensitivity to perceived translucency differences and geometric shape are inherently limited by two factors: our knowledge on how the HVS selects the image regions to deduce translucency; and the availability of proper shape descriptors. For instance, we do not know whether the HVS relies on the information in all visible spikes, or if even a single spike is enough. Nagai et al. [31] have observed that different individuals rely on different image regions to assess translucency that might complicate definition of a robust shape descriptor for translucency differences.

Apart from that, we have used a Buddha shape as an anchor pair. Presence of thin parts in the anchor pair Buddhas might itself have increased sensitivity to anchor pair differences. Additionally, Gigilashvili et al. [18] observed that cross-shape translucency comparison is generally found challenging by observers. Hence, we believe that future studies should consider differently-shaped anchor pairs.

There might be some unintended noise in the data due to the interpretation of the object composition. For some materials the appearance of the sphere proper and its spikes is so different that a couple of observers thought that the spikes were made of a different material and thus, they decided to assess a core sphere only.

Finally, the remarks made by some observers about opacity of optically thick materials opens up a discussion where the conceptual boundary lies between *translucency* and *opacity* (see [19] for further discussion).

We believe future work should evolve towards three objectives: firstly, shape descriptors, which could correlate with detectability of perceived translucency differences, should be developed. We hypothesize that identification of image cues to perceived translucency could facilitate construction of such a descriptor. Subsequently, shape-related effects should be incorporated in translucency difference formulae. Finally, a perceptual translucency space should be constructed that could permit navigation in nearly perceptually uniform units instead of highly perceptually non-uniform absorption and scattering coefficients [16].

5. CONCLUSION

We have conducted psychophysical experiments to identify how object's shape and particularly, presence of thin parts, affect visual detection of perceived translucency differences. We have observed that presence of thin parts in many cases lead to easier detection of translucency differences. However, this impact is difficult to model quantitatively, as the limited knowledge about translucency perception mechanisms does not permit to design proper shape descriptors.

We also found that change in absorption and scattering make more visual impact if their absolute magnitude is smaller. This also reveals that see-through cues, when present, are emphasized over luminance contrast cues leading to the conclusion that perception of see-through and non-see-through translucent objects and materials should be studied independently. This has implications for material design in 3D printing and computer graphics, as well as for psychophysical methods when suprathreshold translucency difference is determined.

ACKNOWLEDGMENT

The work has been funded by the Measuring and Understanding Visual Appearance – MUVApp project of the Research Council of Norway (project #250293). The authors want to thank Tejas Tanksale for his contributions in the stimuli rendering process, Johann Reinhard for computing the distance between surface and medial-axis, and all observers for their voluntary participation in the experiments.

REFERENCES

[1] "ASTM E284-17 standard terminology of appearance." (ASTM International, West Conshohocken, PA, 2017).

[2] J. Beck and R. Ivry, "On the role of figural organization perceptual transparency," Perception & Psychophysics **44**, 585–594 (1988).

[3] R. S. Berns, D. H. Alman, L. Reniff, G. D. Snyder, and M. R. Balonon-Rosen, "Visual determination of suprathreshold color-difference tolerances using probit analysis," Color Res. Appl. **16**, 297–316 (1991).

[4] H. Blum, "A transformation for extracting new descriptors of shape," *Models for the Perception of Speech and Visual Form* (MIT Press, Cambridge, MA, 1967), pp. 362–380.

[5] A. Brunton, C. A. Arikan, T. M. Tanksale, and P. Urban, "3D printing spatially varying color and translucency," ACM Trans. Graph. **37**, 157:1–157:13 (2018).

[6] A. Chadwick, C. Heywood, H. Smithson, and R. Kentridge, "Translucence perception is not dependent on cortical areas critical for processing colour or texture," Neuropsychologia **128**, 209–214 (2019).

[7] A. C. Chadwick, G. Cox, H. E. Smithson, and R. W. Kentridge, "Beyond scattering and absorption: Perceptual unmixing of translucent liquids," J. Vis. **18**, 1–15 (2018).

[8] CIE, *CIE 175: 2006* A framework for the measurement of visual appearance. (Commission Internationale de L'Eclairage, 2006).

[9] D. W. Cunningham, C. Wallraven, R. W. Fleming, and W. Straßer, "Perceptual reparameterization of material properties," *Computational Aesthetics* (Eurographics Digital Library, Geneva, Switzerland, 2007), pp. 89–96.

[10] P. G. Engeldrum, *Psychometric Scaling: A Toolkit for Imaging Systems Development* (Imcotek, Winchester, MA, 2000).

[11] C. Eugène, "Measurement of "total visual appearance": A CIE challenge of soft metrology," *12th IMEKO TC1 and TC7 Joint Symposium on Man, Science and Measurement* (Curran Associates, Red Hook, NY, 2008), pp. 61–65.

[12] R. W. Fleming and H. H. Bülthoff, "Low-level image cues in the perception of translucent materials," ACM Trans. Appl. Perception **2**, 346–382 (2005).

[13] R. W. Fleming, F. Jäkel, and L. T. Maloney, "Visual perception of thick transparent materials," Psychological Sci. **22**, 812–820 (2011).

[14] D. Gigilashvili, L. Dubouchet, M. Pedersen, and J. Y. Hardeberg, "Caustics and translucency perception," *Proc. IS&T Electronic Imaging: Materials Appearance 2020* (IS&T, Springfield, VA, 2020), pp. 033:1–033:6.

[15] D. Gigilashvili, "*On the Appearance of Translucent Objects: Perception and Assessment by Human Observers*," Ph.D. thesis (Norwegian University of Science Technology, Gjøvik, Norway, 2021).

[16] D. Gigilashvili, P. Urban, J. B. Thomas, M. Pedersen, and J. Y. Hardeberg, "Perceptual navigation in absorption-scattering space," *Proc. IS&T CIC29: Twenty-Nineth Color and Imaging Conf.* (IS&T, Springfield, VA, 2021), pp. 328–333.

[17] D. Gigilashvili, F. Mirjalili, and J. Y. Hardeberg, "Illuminance impacts opacity perception of textile materials," *Proc. IS&T CIC27: Twenty-Seventh Color and Imaging Conf.* (IS&T, Springfield, VA, 2019), pp. 126–131.

[18] D. Gigilashvili, J.-B. Thomas, J. Y. Hardeberg, and M. Pedersen, "Behavioral investigation of visual appearance assessment," *Proc. IS&T CIC26: Twenty-Sixth Color and Imaging Conf.* (IS&T, Springfield, VA, 2018), pp. 294–299.

[19] D. Gigilashvili, J. B. Thomas, J. Y. Hardeberg, and M. Pedersen, "On the nature of perceptual translucency," *8th Annual Workshop on Material Appearance Modeling (MAM 2020)* (Eurographics Digital Library, Geneva, Switzerland, 2020), pp. 17–20.

[20] D. Gigilashvili, J.-B. Thomas, J. Y. Hardeberg, and M. Pedersen, "Translucency perception: A review," J. Vis. **21**, 1–41 (2021).

[21] D. Gigilashvili, P. Urban, J. Thomas, J. Y. Hardeberg, and M. Pedersen, "Impact of shape on apparent translucency differences," *Proc. IS&T CIC27: Twenty-Seventh Color and Imaging Conf.* (IS&T, Springfield, VA, 2019), pp. 132–137.

[22] I. Gkioulekas, B. Walter, E. H. Adelson, K. Bala, and T. Zickler, "On the appearance of translucent edges," *Proc. IEEE Conf. on Computer Vision and Pattern Recognition* (IEEE, Piscataway, NJ, 2015), pp. 5528–5536.

[23] I. Gkioulekas, B. Xiao, S. Zhao, E. H. Adelson, T. Zickler, and K. Bala, "Understanding the role of phase function in translucent appearance," ACM Trans. Graph. **32**, 1–19 (2013).

[24] S.-S. Guan and M. R. Luo, "Investigation of parametric effects using small colour differences," Color Res. Appl. **24**, 331–343 (1999).

[25] W. Jakob, "Mitsuba renderer," 2010.

[26] J. J. Koenderink and A. J. van Doorn, "Shading in the case of translucent objects," SPIE **4299**, 312–320 (2001).

[27] M. R. Luo, G. Cui, and B. Rigg, "The development of the CIE 2000 colour-difference formula: CIEDE2000," Color Res. Appl. **26**, 340–350 (2001).

[28] P. J. Marlow, J. Kim, and B. L. Anderson, "Perception and misperception of surface opacity," *Proc. National Academy of Sciences* (National Academy of Sciences, Washington DC, 2017) Vol. 114, pp. 13840–13845.

[29] F. Metelli, "The perception of transparency," Sci. Am. **230**, 90–99 (1974).

[30] I. Motoyoshi, "Highlight–shading relationship as a cue for the perception of translucent and transparent materials," J. Vis. **10**, 1–11 (2010).

[31] T. Nagai, Y. Ono, Y. Tani, K. Koida, M. Kitazaki, and S. Nakauchi, "Image regions contributing to perceptual translucency: A psychophysical reverse-correlation study," i-Perception **4**, 407–428 (2013).

[32] Z. Pizlo, "Perception viewed as an inverse problem," Vis. Res. **41**, 3145–3161 (2001).

[33] D. Rebain, B. Angles, J. Valentin, N. Vining, J. Peethambaran, S. Izadi, and A. Tagliasacchi, "LSMAT least squares medial axis transform," *Computer Graphics Forum* (Wiley Online Library, Hoboken, NJ, 2019), pp. 5–18.

[34] M. Sawayama, Y. Dobashi, M. Okabe, K. Hosokawa, T. Koumura, T. Saarela, M. Olkkonen, and S. Nishida, "Visual discrimination of optical material properties: a large-scale study," *BioRxiv* (Cold Spring Harbor Laboratory, 2019), No. 800870, pp. 1–34.

[35] M. Singh and B. L. Anderson, "Perceptual assignment of opacity to translucent surfaces: The role of image blur," Perception **31**, 531–552 (2002).

[36] "The Stanford 3D Scanning Repository," (Stanford University Computer Graphics Laboratory, 1994).

[37] S. S. Stevens, "The psychophysics of sensory function," Am. Sci. **48**, 226–253 (1960).

[38] P. Urban, M. Fedutina, and I. Lissner, "Analyzing small suprathreshold differences of LCD-generated colors," JOSA A **28**, 1500–1512 (2011).

[39] P. Urban, T. M. Tanksale, A. Brunton, B. M. Vu, and S. Nakauchi, "Redefining A in RGBA: Towards a standard for graphical 3D printing," ACM Trans. Graph. **38**, 1–14 (2019).

[40] B. M. Vu, P. Urban, T. M. Tanksale, and S. Nakauchi, "Visual perception of 3D printed translucent objects," *Proc. IS&T CIC24: Twenty-fourth Color and Imaging Conf.* (IS&T, Springfield, VA, 2016), pp. 94–99.

[41] B. Xiao, B. Walter, I. Gkioulekas, T. Zickler, E. Adelson, and K. Bala, "Looking against the light: How perception of translucency depends on lighting direction," J. Vis. **14**, 1–22 (2014).

[42] B. Xiao, S. Zhao, I. Gkioulekas, W. Bi, and K. Bala, "Effect of geometric sharpness on translucent material perception," J. Vis. **20:7**, 1–17 (2020).